Background resistivity model from seismic velocities

Dieter Werthmüller, Anton M. Ziolkowski, and David A. Wright, University of Edinburgh*

Summary

Joint analysis of seismic and electromagnetic data is difficult because the data sets lack a common physical parameter, and rock physics is usually applied to link the two methods via porosity. However, rock physics parameters are not well known in near field exploration, and estimates are likely to have large errors associated with them. In this work, we use a set of rock physics relations to link velocity to resistivity. Which relation is used is a function of depth and lithology, or seismic velocity, and the relations itself are a function of depth. We then estimate the uncertainty of our model. We apply our methodology to seismic velocities from the North Sea, were we show that the background resistivities of a field can be modelled by (1) calibrating rock physics models for different lithologies on a well log from an adjacent field (including their depth-trends), and (2) calculating the corresponding uncertainty. This method is a useful tool for generating a more realistic resistivity background model for electromagnetic inversions, where resistivities are given as probability density functions.

Introduction

Joint analysis of seismic and electromagnetic data is of great interest with the commercialization of marine Controlled-Source EM (CSEM) methods in the last decade. A possible approach to combine these data is to obtain resistivity estimates from seismic data. This usually involves rock physics as a link, as there is no common physical parameter (Ziolkowski and Engelmark, 2009). There are two steps: first, to transform velocity to porosity and, second, to transform porosity to resistivity. Carcione et al. (2007) presented an extensive overview of cross-property relations specific to seismic and electromagnetic data. Engelmark (2010) emphasizes the importance of background (shale) modelling for EM inversions, and the depth-dependence of rock physics models. However, any rock physics model has an extrinsic uncertainty from the parameters, and an intrinsic uncertainty from the model. Chen and Dickens (2009) present a strategy to calculate these uncertainties. Werthmüller et al. (2012) combined these methods, rock physics modelling, depth-trend, and uncertainty analysis, and applied their methodology to well data from the North Sea Harding Field (Beckly et al., 2003), where a successful electromagnetic repeatability experiment had been carried out by Ziolkowski et al. (2010).

We extend the work by Werthmüller et al. (2012) for deeper and shallower sections than the extent of the well measurements, and apply our model to a seismic velocity slice to gain a resistivity background model for the whole subsurface, including their uncertainties.

First, we briefly recap the methodology and explain our extension to shallower and deeper sections, where we use depth, velocity, and picked horizons as discrimination criteria. We then apply this extended methodology to well data for comparison, and finally to a 2D seismic velocity slice.

Rock Physics Model

Elastic and electromagnetic waves share no physical parameters and have very different spatial resolution (e.g. Ziolkowski and Engelmark, 2009). This fundamental obstacle to combining these two types of data is usually tackled in two steps: first, velocities are transformed into porosities and, second, porosities are transformed into resistivities. Carcione et al. (2007) give an extensive overview of cross-property relations between elastic and electromagnetic waves. These and more rock physics models are presented in Mavko et al. (2009), and all transformations mentioned in this section can be found in that book.

We use a Gassmann-based relation (f_G) for the transformation from velocity v to porosity ϕ, and the self-similar model (f_s) for the transformation from porosity ϕ to resistivity ρ, as described in more detail in Werthmüller et al. (2012). The resistivity resulting from the rock physics calculation, ρ_{rp}, is hence given by

$$\begin{aligned}\rho_{\mathrm{rp}} &= f_s(\rho_{\mathrm{s}}, \rho_{\mathrm{f}}, \mathrm{m}, \phi)\ , \quad \text{where} & (1)\\ \phi &= f_G(K_{\mathrm{s}}, K_{\mathrm{f}}, G_{\mathrm{s}}, \delta_{\mathrm{s}}, \delta_{\mathrm{f}}, v)\ , & (2)\end{aligned}$$

ρ_s and ρ_f are the resistivities of the solid and the fluid fraction respectively, m is the cementation exponent, ϕ is porosity, K_s and K_f are the bulk moduli of the solid and the fluid fraction respectively, G_s is the shear modulus of the solid fraction, δ_s and δ_f are the density of the solid and the fluid fraction respectively, and v is the P-wave velocity.

Uncertainty Analysis

Chen and Dickens (2009) describe a methodology to account for the uncertainties related to rock physics parameters and the rock physics model itself. They describe the rock physics model as gamma distribution in a Bayesian framework, with a defined error E, and the rock physics parameters as distributions,

$$f(\rho|\theta) = \frac{\beta^{\alpha}\rho^{\alpha-1}}{\Gamma(\alpha)}\exp\left(-\beta\rho\right)\ , \qquad (3)$$

where θ is a vector containing all model parameter distributions, $\alpha = 1/\mathrm{E}^2$, and $\beta = (\alpha-1)/\rho_{\mathrm{rp}}$. Here, ρ_{rp} is one realization of

DOI http://dx.doi.org/10.1190/segam2012-0696.1

the rock physics model in Equations 1 and 2 with a random set of model parameters. To get the probability density function (pdf) of the whole range of possible parameters, one has to integrate over all values,

$$f(\rho) = \int f(\rho|\theta) f(\theta) d\theta \ , \tag{4}$$

for this we used a Markov Chain Monte Carlo sampler, as suggested by the authors. However, our approach differs in that we describe *all* fixed input parameters as uniform distributions around the defined value with an error $E = 5$ %, and we define the distribution of the velocity *from the data themselves*, as shown in Figure 1. The distribution is defined as the difference between the log values and the values of the smoothed log, $v(z) - v^s(z)$, where v^s is smoothed with a Hanning window over 320 log-samples ($\approx$ 48.8 m). The smoothing is justified by the expected resolution of our CSEM data. This method accounts for the variability of velocities, and the resulting distribution is thought to be wider than errors in seismic velocities resulting from acquisition and processing of seismic data. The pdf of this data distribution is then found with a kernel density estimation, here with a Gaussian kernel. The result of this methodology is resistivity ρ as a pdf for any given set of model parameters, instead a single value ρ_{rp}, as shown schematically in Figure 2. The figure shows the distribution for a case where the rock physics model yields a resistivity $\rho_{\mathrm{rp}} \approx 1.42\ \Omega$m. The blue line is the pdf for the resistivity values, where the green line is the mode, and the red lines correspond to the standard deviation σ in a normal distribution, as they include the area that contains 68.2 % of all realisations.

Model selection

The idea behind cross-property relations between elastic and electromagnetic waves in hydrocarbon exploration is to get resistivity values from seismic data. The ideal model would predict the correct resistivities at any point. However, this ideal model has yet to be found. One reason is that shales, sandstones and limestones can have very different rock characteristics like, e.g., the resistivity of the solid fraction ρ_s. Furthermore we usually assume conductive brine as the pore space filling liquid, and hence no rock physics model will predict the correct resistivities in a hydrocarbon bearing target. All parameters of a rock physics model are a function of, amongst other things, pressure and temperature, and hence, to a first order approximation, a function of depth. Engelmark (2010) showed that the change of brine resistivity with changing temperature is likely to be the major influence.

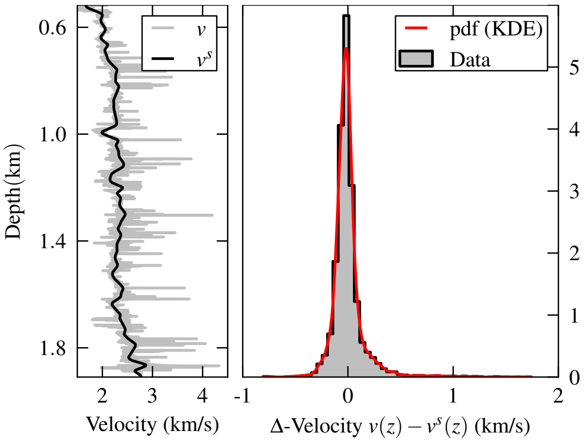

Figure 1: *Estimation of P-wave velocity distribution from well log data (Well 9/23b-8), using a Gaussian Kernel Density Estimation.*

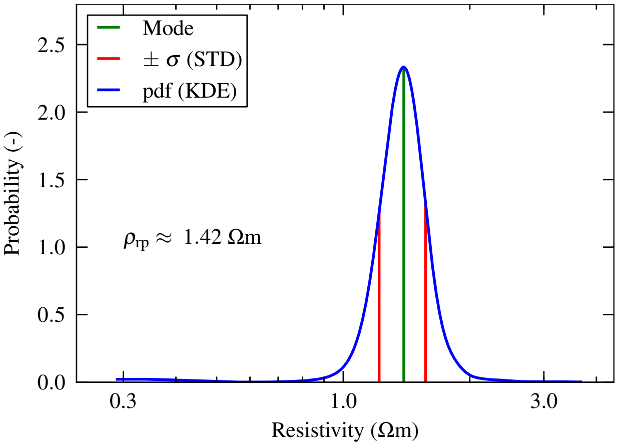

Figure 2: *Example probability density function. The rock physics model yields $\rho_{rp} \approx 1.42\ \Omega m$. The uncertainty analysis yields $\rho_{mode} \approx 1.39\ \Omega m$, and $\rho_{\pm\sigma} \approx 1.21; 1.59\ \Omega m$.*

We present here an approach with four different rock physics relations. The main model is a depth-dependent shale model, following the approach presented by Engelmark (2010). The resistivity of brine, ρ_f, decreases with increasing temperature, and hence with increasing depth. In addition we apply as well a linear depth trend for the bulk and shear moduli of the solid fraction, G_s and K_s.

The first exception (1) from this model is for depths shallower than 750 m, the unconsolidated part, were we use a sand model without depth-dependence. The second exception (2) is an example of how additional information can be incorporated into the work flow: The grid sandstone is a thick sand formation at roughly 1 km depth. We apply a different sand model within this layer.

The seismic velocities within our area of interest lie roughly between 1.5 km/s and 6.0 km/s. Even with a depth trend, a rock physics model is not able to hold true over that wide range of velocities. The third exception (3) is therefore an adjusted model

DOI http://dx.doi.org/10.1190/segam2012-0696.1

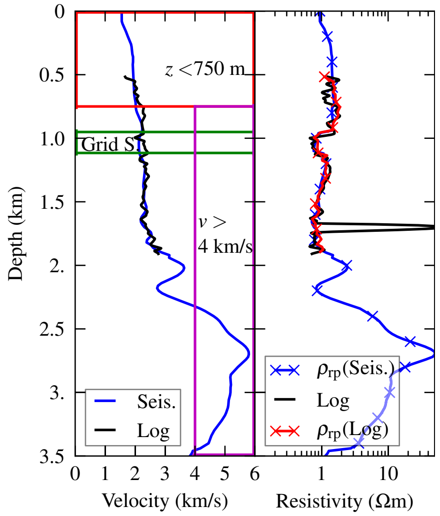

Figure 3: *Model selection: The depth-dependent shale model is used except for (red) depths $z < 740$ m, (green) the Grid sandstone formation, and (magenta) for velocities $v > 4.0$ km/s.*

for velocities over 4.0 km/s.

The cementation factor m is in all four models a function of porosity ϕ, as proposed by Engelmark (2010).

We calibrate all four models with well logs from Well 9/23b-8 in Harding South, as shown in Figure 3. The black and the blue lines on the left are the velocities from the well log and the seismic data, respectively. On the right side, the black line is the resistivities from the well log. The blue and the red lines with crosses are the outcomes of the cross-property transformation (ρ_{rp}) from the velocities of the well log and the seismic data, respectively. The models described above are indicated in red (1), green (2), and magenta (3); the main model applies everywhere else. The results show first of all the good fit of the seismic velocities to the well log velocities. But most importantly, the rock physics model can predict the resistivities, if there are no hydrocarbons present, to a satisfying degree. The shortcoming is that we do not have any control shallower than 0.5 km or deeper than 2 km, as there are no well logs.

Near Field Exploration Simulation

We simulate a near field exploration situation, where we have knowledge from a nearby oilfield, and would like to extrapolate this knowledge to an exploration target. We use the calibration from Well 9/23b-8 from Harding South, as shown in Figure 3; the result is shown again in the leftmost panel of Figure 4a. The same model is then applied to the wells of Harding Central, to test the robustness of our approach. It shows that the model nicely predicts the resistivities for the areas without hydrocarbons. Figure 4a is an update with the presented four-model approach of the results in Werthmüller et al. (2012). It shows that we can handle big anomalies, like a thick sand layer, if we have interpretations from the seismic data at hand. It further shows that most of the well log resistivity measurements from Harding central fall within $\pm\,\sigma$ (68.2 %) of the pdf. When taking the whole range from the pdf the entire well log measurements, excluding the hydrocarbon bearing formations, fall within the predicted resistivity distribution.

Application to Seismic Data

We apply the described and tested methodology to an interpolated slice through a seismic velocity cube along the line of the CSEM repeatability test-case described in Ziolkowski et al. (2010). The slice is shown in Figure 5a, with some major horizons and the velocity well log of Well 9/23b-7. The black vertical lines indicate the start- and end-points of the EM measurements. Figure 5b shows the result of the rock physics transformation, where the modes of the probability density functions are plotted. The similarity to the seismic velocities is obvious and logical, as one is derived from the other. However, considering that the background resistivity model is a pdf at each point, the model becomes much more independent of the seismic velocities. The resistivities of $\pm\,\sigma$ are shown in Figures 5c and 5d.

Conclusions

Using well log data and seismic velocities, we present an integrated approach for estimating a background resistivity model from seismic velocities, applying and extending known methods. The approach employs depth dependent petrophysical cross-property relations with a set of different parameters, and uncertainty analysis of both the data and the model. Our near field exploration example shows that this methodology yields a good estimate of background resistivities away from our control point, and hence provides an excellent starting point for any CSEM inversion routine. Using a probability distribution instead of fixed values for the background model decreases the influence of unwanted bias that originates from the different physical properties of the seismic and EM methods.

This abstract presents a work flow, where the main blocks are (a) rock physics model, (b) model selection, and (c) uncertainty analysis. These blocks can be adjusted as necessary, e.g. the transformations f_G and f_s in Equations 1 and 2 could be replaced with transformations other than the Gassmann relation and the self-similar model. Similarly, one could include more information from the seismic interpretation, or adjust the errors in the parameters and the model of the uncertainty analysis.

Acknowledgements

We thank PGS for funding the research and the Harding partners, BP and Maersk, for permission to use the data.

DOI http://dx.doi.org/10.1190/segam2012-0696.1

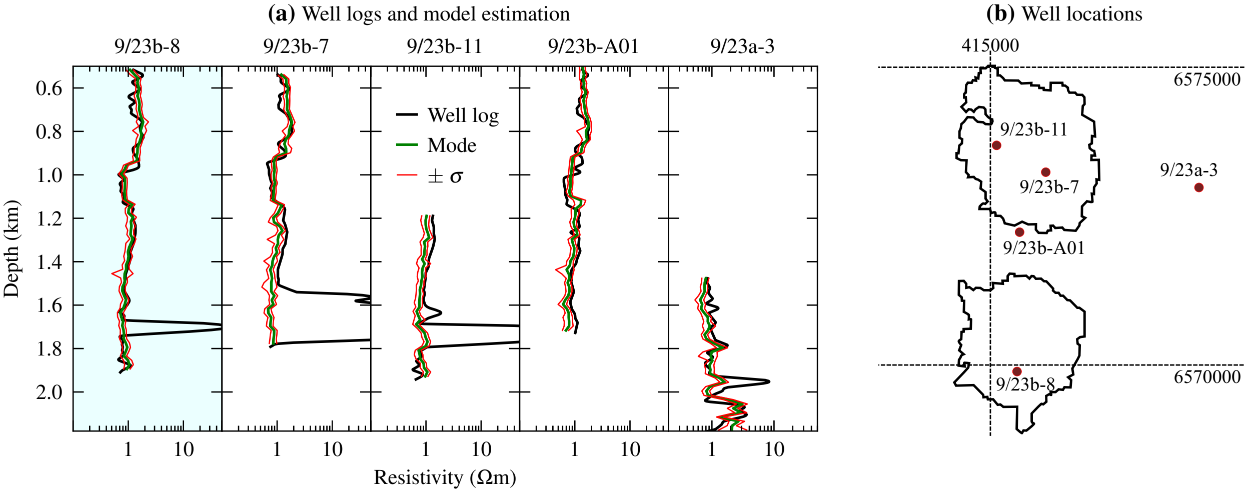
(a) Well logs and model estimation

(b) Well locations

Figure 4: *(a) The model is calibrated with Well 9/23b-8 from Harding South, and the same parameters are applied to wells of Harding Central. The actual (smoothed) well measurements are shown in black, the modes of the rock physics and uncertainty analysis are shown in green, and in red ± σ of the result. (b) Location of the wells.*

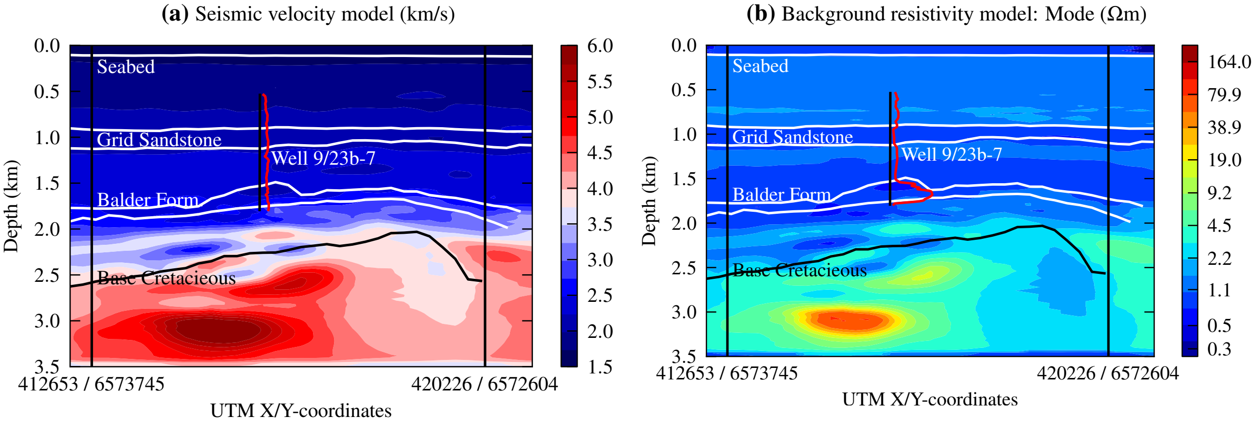
(a) Seismic velocity model (km/s)

(b) Background resistivity model: Mode (Ωm)

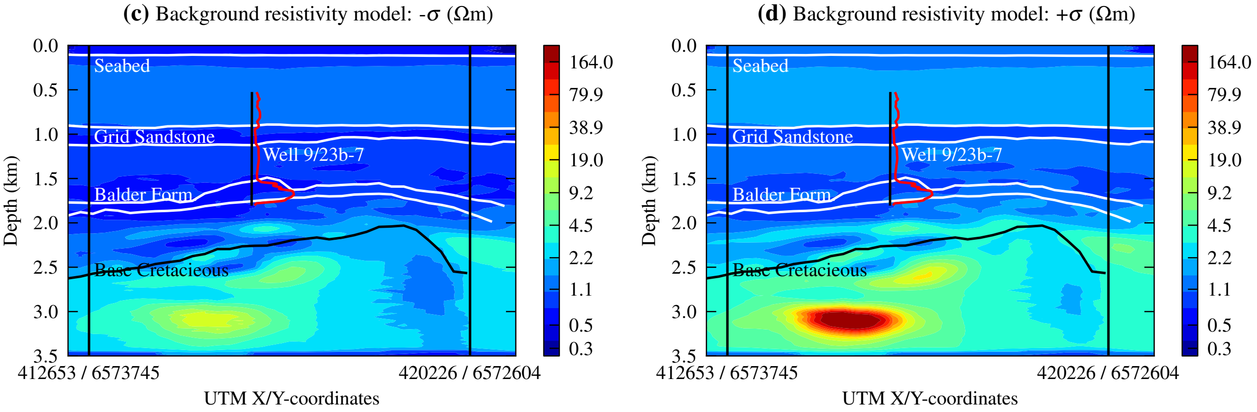
(c) Background resistivity model: -σ (Ωm)

(d) Background resistivity model: +σ (Ωm)

Figure 5: *(a) Seismic velocity slice. (b) Mode of background resistivity model from the rock physics and uncertainty analysis, (c) & (d) background resistivity of ± σ (corresponding to the red lines in Figure 4a).*

DOI http://dx.doi.org/10.1190/segam2012-0696.1

http://dx.doi.org/10.1190/segam2012-0696.1

EDITED REFERENCES

REFERENCES

Beckly, A. J., T. Nash, R. Pollard, C. Bruce, P. Freeman, and G. Page, 2003, The Harding field, block 9/23b, *in* United Kingdom oil and gas fields commemorative millennium volume: Geological Society Publishing House, 283–290, doi:10.1144/GSL.MEM.2003.020.01.01.

Carcione, J. M., B. Ursin, and J. I. Nordskag, 2007, Cross-property relations between electrical conductivity and the seismic velocity of rocks: Geophysics, **72**, no. 5, E193–E204.

Chen, J., and T. A. Dickens, 2009, Effects of uncertainty in rock-physics models on reservoir parameter estimation using seismic amplitude variation with angle and controlled-source electromagnetics data: Geophysical Prospecting, **57**, 61–74.

Engelmark, F., 2010, Velocity to resistivity transform via porosity: 80th Annual International Meeting, SEG, Expanded Abstracts, 2501–2505.

Mavko, G., T. Mukerji, and J. Dvorkin, 2009, The rock physics handbook: Cambridge University Press.

Werthmüller, D., A. M. Ziolkowski, and D. A. Wright, 2012, Uncertainty analysis of velocity to resistivity transforms for near field exploration: 74th Conference and Exhibition, EAGE, Extended Abstracts, A014.

Ziolkowski, A., and F. Engelmark, 2009, Use of seismic and EM data for exploration, appraisal and reservoir characterization: CSPG CSEG SWLS Joint Convention, Abstracts, 424–427.

Ziolkowski, A. M., R. Parr, D. A. Wright, V. Nockles, C. Limond, E. Morris, and J. Linfoot, 2010, Multi-transient electromagnetic repeatability experiment over the North Sea Harding field: Geophysical Prospecting, **58**, 1159–1176.

DOI http://dx.doi.org/10.1190/segam2012-0696.1